超越平均场理论研究原子核的单粒子性质

曹李刚

华北电力大学

第十五届全国核结构大会
广西·桂林, 2014.10.25-28

Contents of this talk

- Motivation of this work
- Method
- Results and discussion
- Summary and perspective

Motivation of this work

self-consistent mean field theory or the nuclear energy density functional theory
starts from an effective NN interactions
(properties of nuclear matter and finite nuclei)

such as: zero-range Skyrme force
finite-range Gogny force
relativistic Lagrangian

very successful → bulk properties
Binding energy(0.581MeV), Radii(0.03fm)
S. Goriely, N. Chamel, et. al., PRL 102(2009)152503
stable nuclei and exotic nuclei

Giant resonances(monopole, dipole, Pygmy dipole…)

limitations of NEDFT

- Widths of GRs.
- Single-particle states and their spectroscopic factors

$$\left(\frac{d\sigma}{d\Omega}\right)_{\text{exp}} = S^2 \left(\frac{d\sigma}{d\Omega}\right)_{\text{DWBA}}$$

NIKHEF NPA 553, 297c (1993)

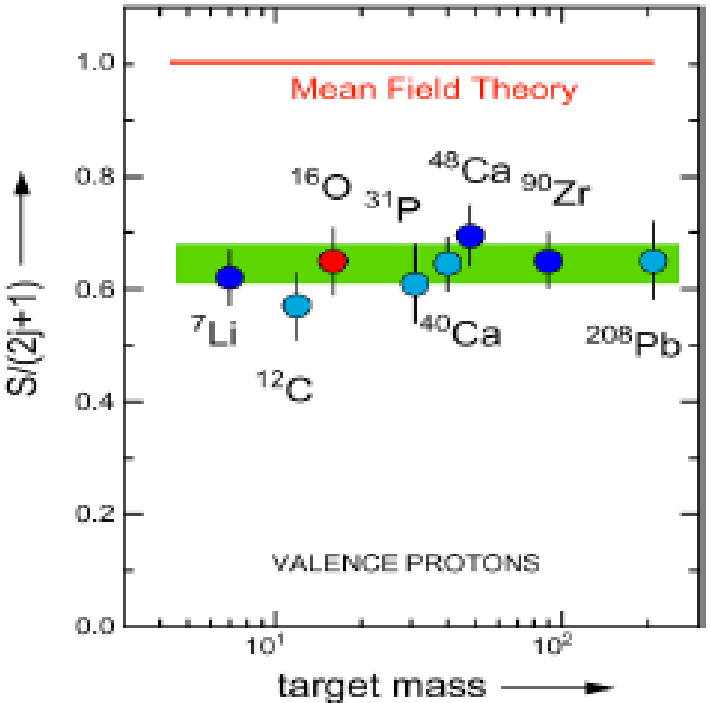

Particle-vibration coupling (PVC) method for nuclei

In the Dyson equation

$$G(\omega) = G_0(\omega) + G_0(\omega)\Sigma(\omega)G(\omega)$$

2nd order PT:

$\varepsilon + <\Sigma(\varepsilon)>$

we assume the self-energy is given by the coupling with RPA vibrations

$$\Sigma(\vec{r},\vec{r}';\omega) = \int d_3r_1 d_3r_2 \; v(\vec{r},\vec{r}_1)\Pi^{(\mathrm{RPA})}(\vec{r}_1,\vec{r}_2;\omega)v(\vec{r}_2,\vec{r}')$$

In a diagrammatic way

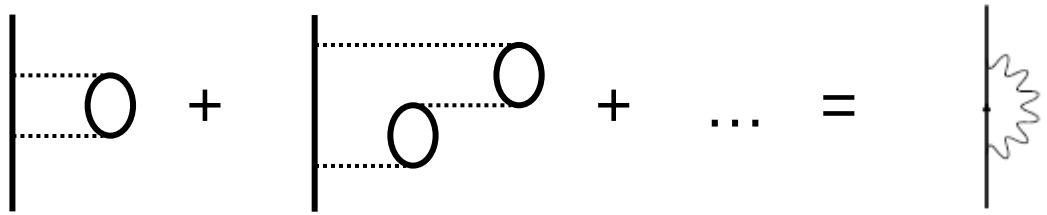

Particle-vibration coupling

Density vibrations are the most prominent feature of the low-lying spectrum of spherical systems

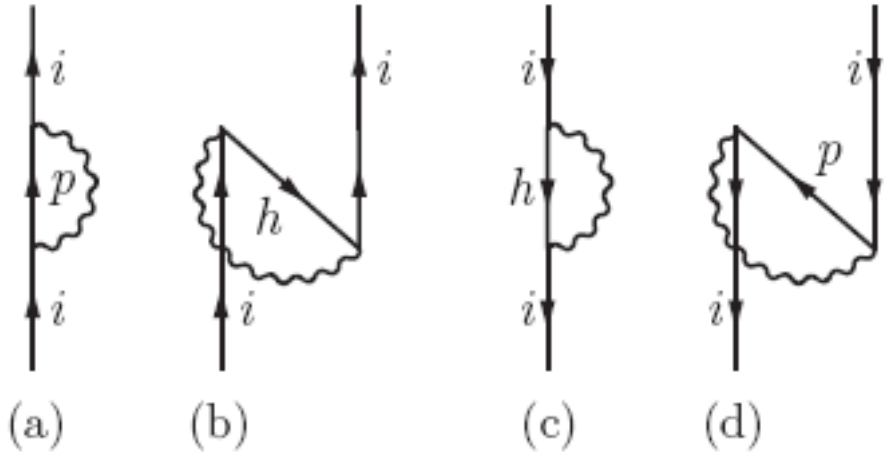

FIG. 1. The four diagrams associated with the single-nucleon self-energy. See the text for details.

$$\Sigma_i(\omega) = \frac{1}{2j_i+1}\left(\sum_{nL,\ p>F}\frac{|\langle i||V||p,nL\rangle|^2}{\omega-\varepsilon_p-\omega_{nL}+i\eta}\right.$$
$$\left.+\sum_{nL,\ h<F}\frac{|\langle i||V||h,nL\rangle|^2}{\omega-\varepsilon_h+\omega_{nL}-i\eta}\right),$$

- APPROXIMATIONS AND PHENOMENOLOGICAL INPUTS HAVE BEEN OFTEN INTRODUCED IN THESE THEORIES.

E.g., in the original Bohr-Mottelson model, the phonons are treated as fluctuations of the mean field δU and their properties are taken from experiment.

$$\langle n_\alpha = 1,\ j' | \delta U | j \rangle =$$

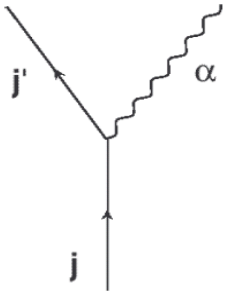

	BG 80	LK 81	BBDM83	WML 81	SRK 83
ν	1.29	1.37	1.33	1.27	1.30
ν^{-1}	1.62	1.68	1.41		
π		1.71	1.29	1.37	1.43
π^{-1}		1.43	1.61		1.49
	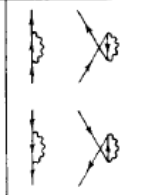	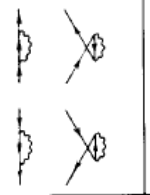	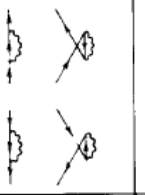	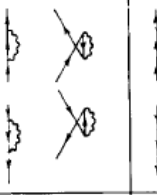	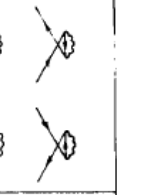
int. j	50 MeV (HF box) $\lambda^\pi = 0^+, 1^-, \ldots, 4^+$ $(\tau = 0+1)$ HF r-space	$0\hbar\omega, 1\hbar\omega, 2\hbar\omega$ $\lambda^\pi = 0^+, 2^+, \ldots, 8^+$ (HO) $1^+, 2^-, \ldots, 4^-$ $(\tau = 0+1,\ \sigma = 0+1)$ obs	ϵ_h unrestr $\epsilon_p \leq 40$ MeV $\lambda^\pi \leq 2^+, 3^-, \ldots, 10^+$ $(\tau = 0)$ HF Skyrme III (box)	2 shells above / below ϵ_F $\lambda^\pi = 0^+, 2^+, \ldots, 13^-$, $1^+ 2^-, \ldots, 14^-$ $(\tau = 0+1;\ \sigma = 0+1)$ scaled WS(m*/m=.7)	$0\hbar\omega$-$3\hbar\omega$ WS $(\tau = 0+1;\ \sigma = 0+1)$ scaled WS(m/m=.7)
V	Skyrme III	Landau-Migdal	mult-mult. (du/dr) self cons. χ	Landau-Migdal plus π and ρ exch. potls	M3Y, renormalized particle hole int.

C. Mahaux *et al.*, Phys. Rep. 120, 1 (1985)

- QUALITATIVELY, ALL THE CALCULATIONS HAVE PREDICTED A REDUCTION OF THE S.P. GAP E.G. IN ^{208}Pb. (m*/m from ≈ 0.7 to 1).

•Pioneering Skyrme calculation by V. Bernard and N. Van Giai in the 80s (neglect of the velocity-dependent part of V_{eff} in the PVC vertex).

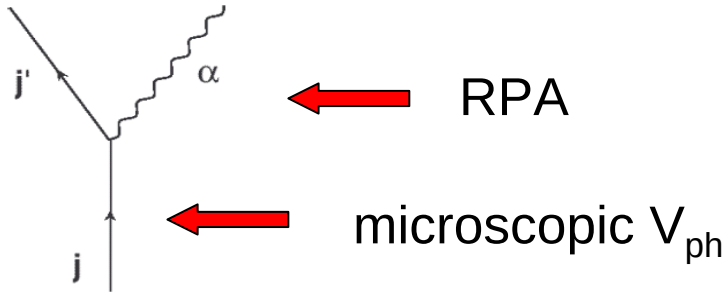

- Microscopic calculations are now feasible. One starts from Hartree or Hartree-Fock with V_{eff} and add PVC on top of it. All is calculated using the same Hamiltonian or EDF consistently.

G. Colò, L. Cao, N. Van Giai, L. Capelli
Comp. Phys. Comm. 184, 142 (2013).

A consistent study within the Skyrme framework

We have implemented a version of PVC in which the treatment of the coupling is exact, namely we do not wish to make any approximation in the vertex.

$$\langle i||V||j,nL\rangle = \sqrt{2L+1}\sum_{\rm ph} X^{nL}_{\rm ph}V_L(ihjp) + (-)^{L+j_h-j_p}Y^{nL}_{\rm ph}V_L(ipjh)$$

The whole phonon wavefunction is considered, and all the terms of the Skyrme force enter the p-h matrix elements

$$V_L(ihjp) = \sum_{\text{all } m}(-)^{j_j-m_j+j_h-m_h}\langle j_i m_i j_j m_j|LM\rangle\langle j_p m_p j_h m_h|LM\rangle\langle j_i m_i, j_h m_h|V|j_j m_j, j_p m_p\rangle$$

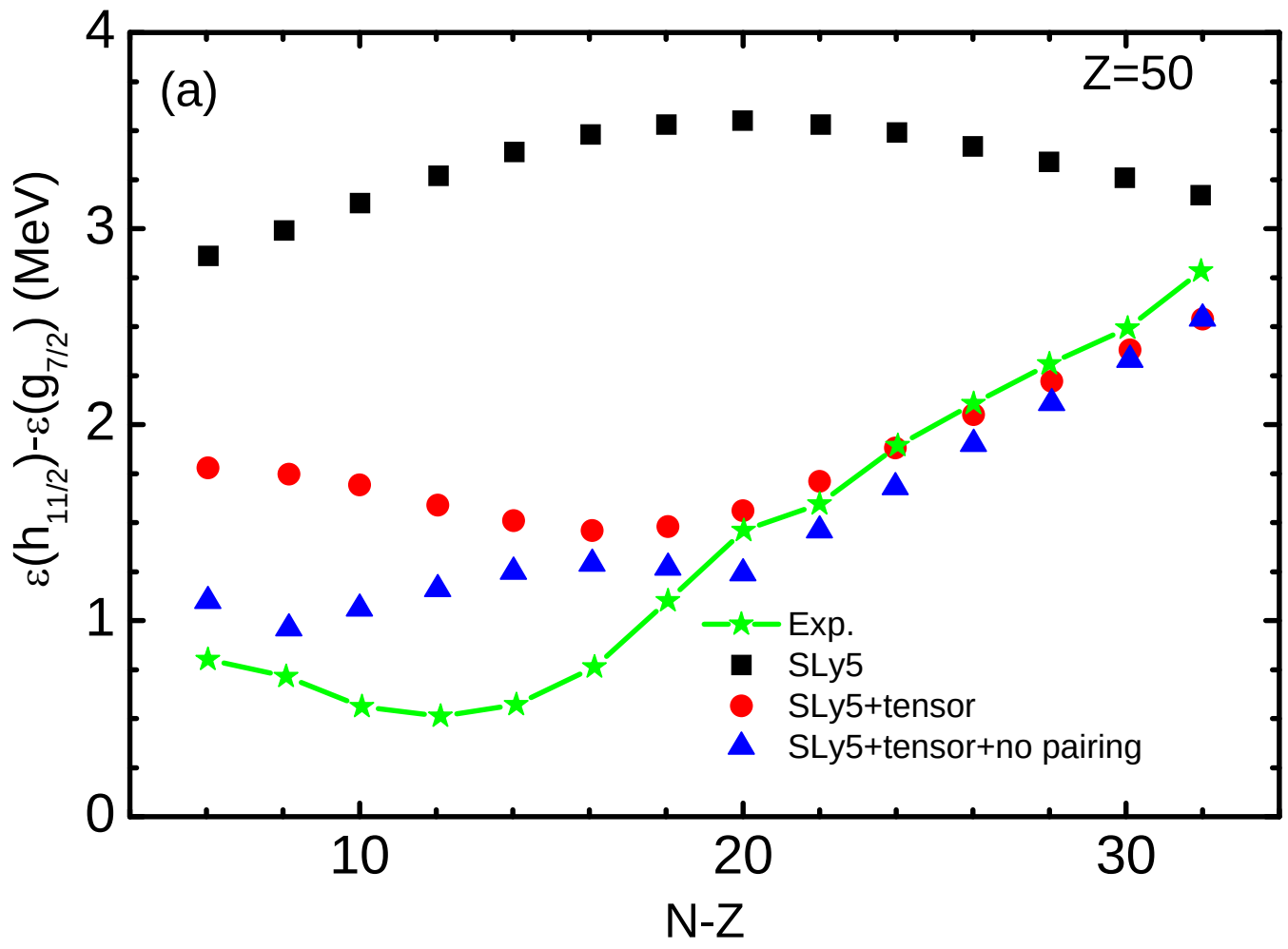

SLy5
G. Colo, et. al.
PLB646(2007)227

$\alpha_c = 80.2 MeVfm^5$

$\beta_c = -48.9 MeVfm^5$

$\alpha_T = -170 MeVfm^5$

$\beta_T = 100 MeVfm^5$

$\alpha = -89.8 MeVfm^5$

$\beta = 51.1 MeVfm^5$

$T = 888.0 MeVfm^5$

$U = -408.0 MeVfm^5$

$$U_{s.o.}^{p} = \frac{W_0}{2r}\left(2\frac{d\rho_p}{dr} + \frac{d\rho_n}{dr}\right) + \left(\alpha\frac{J_p}{r} + \beta\frac{J_n}{r}\right)$$

^{120}Sn neutron spin-saturated state
$J_n = 0$

$1g_{9/2}, \quad J_p > 0, \alpha = -89.8 MeVfm^5 < 0 \quad U_{s.o.}^{p} \uparrow \quad \varepsilon_{h11/2} \downarrow \quad \varepsilon_{g7/2} \uparrow$

Results and discussion

I. Single-particle states

Cao LG, et.al., Phys.Rev. C89, 044314 (2014)

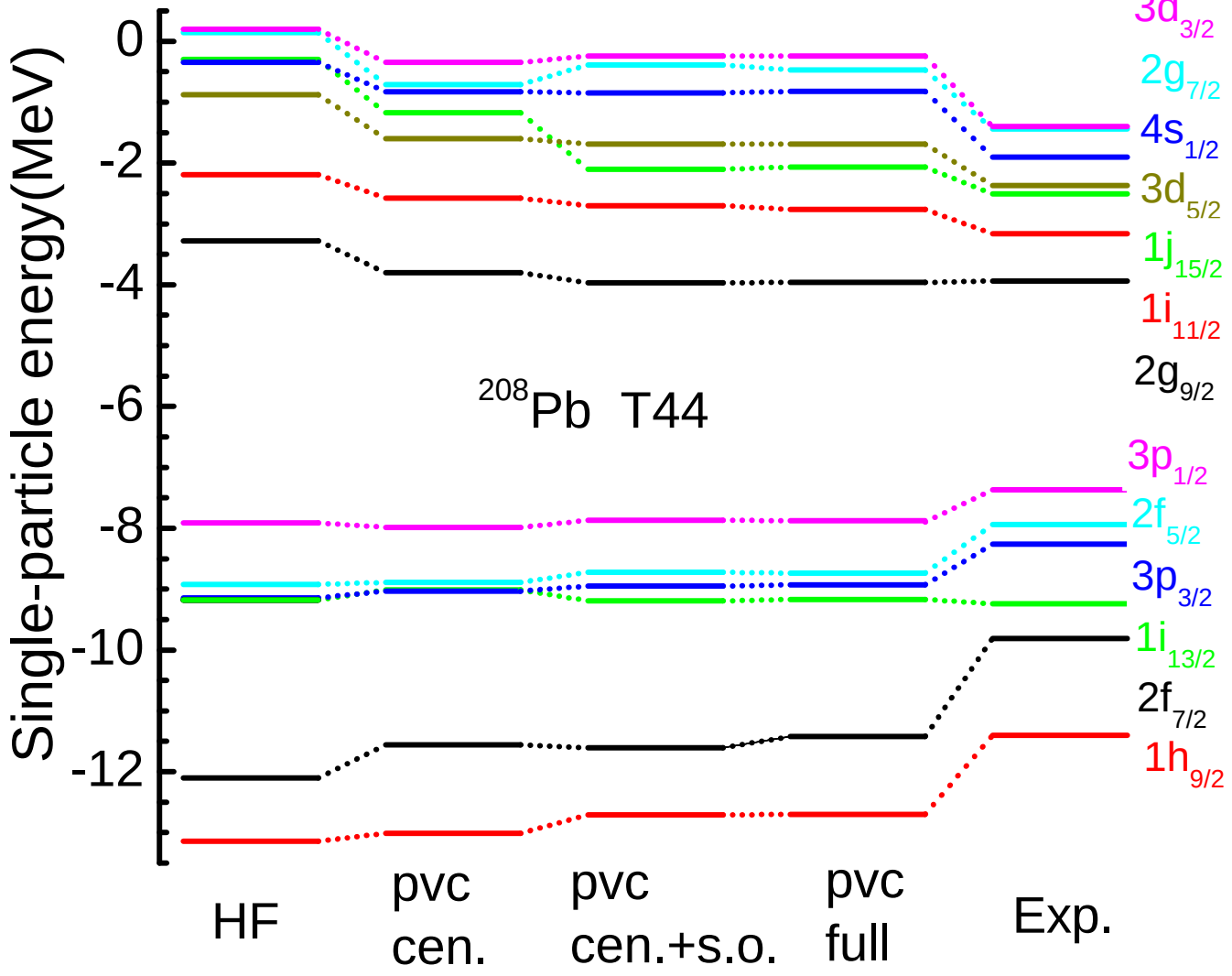

The values of σ are 1.421, 1.002, 0.907, 0.873 for T44 .

Cao LG, et.al., Phys.Rev. C89, 044314 (2014)

TABLE I. Energies and reduced transition probabilities of the low-lying states in ^{40}Ca and ^{208}Pb obtained by HF+RPA with SLy5 and T44 parameter sets. The values in parentheses are the results obtained without the contribution of the tensor force. The experimental data are from Ref. [33].

	J^π	Theory				Experiment	
		SLy5		T44			
		Energy (MeV)	$B(EL,0\rightarrow L)$ (e^2 fm^{2L})	Energy (MeV)	$B(EL,0\rightarrow L)$ (e^2 fm^{2L})	Energy (MeV)	$B(EL,0\rightarrow L)$ (e^2 fm^{2L})
^{40}Ca	3^-	3.225(3.822)	$0.884(1.285)\times 10^4$	1.366(1.508)	$0.852(1.280)\times 10^4$	3.74	1.18×10^4
^{208}Pb	2^+	5.155(4.934)	$3.065(2.858)\times 10^3$	4.549(5.105)	$2.478(2.785)\times 10^3$	4.09	4.09×10^3
	3^-	3.585(3.671)	$4.928(6.374)\times 10^5$	3.337(3.629)	$5.739(5.523)\times 10^5$	2.61	6.21×10^5
	4^+	5.760(5.417)	$1.395(1.256)\times 10^7$	4.655(5.684)	$0.782(1.382)\times 10^7$	4.32	1.29×10^7
	5^-	4.022(4.560)	$2.881(4.898)\times 10^8$	3.977(4.092)	$3.796(2.443)\times 10^8$	3.19	4.62×10^8
		4.507(5.589)	$0.748(1.642)\times 10^8$	4.532(5.021)	$0.345(1.929)\times 10^8$	3.71	3.30×10^8

II. Effective mass

Cao LG, et.al., Phys.Rev. C89, 044314 (2014)

$$\frac{m^*}{m} = \frac{\widetilde{m}}{m} \times \frac{\overline{m}}{m}$$

$$\frac{\widetilde{m}}{m} = \left(1 + \frac{m}{\hbar^2 k}\frac{\partial M}{\partial k}\right)^{-1} \qquad \frac{\overline{m}}{m} = \left(1 - \frac{\partial M}{\partial E}\right)$$

TABLE V: The calculated effective mass for neutron states in ^{208}Pb in various approximations. The results are obtained by using SLy5 and T44 parameter sets.

	HF	pvc central		pvc central+S.O.		pvc full	
	m^*_k	m^*_e	m^*	m^*_e	m^*	m^*_e	m^*
SLy5	0.839	1.156	0.968	1.198	1.002	1.229	1.028
T44	0.841	1.157	0.973	1.200	1.009	1.235	1.038

II. Spectroscopic factor

$$S_\alpha^\lambda = \left(1 - \frac{\partial \Sigma_\alpha}{\partial \varepsilon}\right)^{-1}_{\varepsilon=\varepsilon_\alpha^\lambda}.$$

TABLE IV: The energies and spectroscopic factors of the single-particle states in ^{208}Pb in various approximations. The results are obtained by using SLy5 and T44 parameter sets. The experimental data are taken from Ref.[31, 32].

		HF	pvc central		pvc central+S.O.		pvc full			Spectroscopic factors	
		$\varepsilon^{(0)}$	$\Delta\varepsilon_i$	ε_i	$\Delta\varepsilon_i$	ε_i	$\Delta\varepsilon_i$	ε_i	ε_i^{exp}	S_i^{th}	S_i^{exp}
T44	$3d_{3/2}$	0.20	-0.55	-0.35	-0.44	-0.24	-0.44	-0.24	-1.40	0.895	1.09
	$2g_{7/2}$	0.14	-0.85	-0.71	-0.53	-0.39	-0.61	-0.47	-1.44	0.832	1.05
	$4s_{1/2}$	-0.35	-0.48	-0.83	-0.50	-0.85	-0.47	-0.82	-1.90	0.896	0.98
	$3d_{5/2}$	-0.88	-0.72	-1.60	-0.81	-1.69	-0.81	-1.69	-2.37	0.855	0.98
	$1j_{15/2}$	-0.30	-0.87	-1.17	-1.80	-2.10	-1.77	-2.07	-2.51	0.583	0.58
	$1i_{11/2}$	-2.19	-0.39	-2.58	-0.51	-2.70	-0.57	-2.76	-3.16	0.884	0.86
	$2g_{9/2}$	-3.28	-0.52	-3.80	-0.69	-3.97	-0.68	-3.96	-3.94	0.877	0.83
	$3p_{1/2}$	-7.91	-0.08	-7.99	0.04	-7.87	0.03	-7.88	-7.37	0.905	0.90
	$2f_{5/2}$	-8.92	0.03	-8.89	0.19	-8.72	0.18	-8.74	-7.94	0.888	0.60
	$3p_{3/2}$	-9.14	0.11	-9.03	0.19	-8.95	0.21	-8.93	-8.26	0.844	0.88
	$1i_{13/2}$	-9.18	0.17	-9.01	-0.01	-9.19	0.01	-9.17	-9.24	0.903	0.91
	$2f_{7/2}$	-12.10	0.54	-11.56	0.49	-11.61	0.68	-11.42	-9.81	0.580	0.95
	$1h_{9/2}$	-13.14	0.13	-13.01	0.43	-12.71	0.44	-12.70	-11.40	0.831	0.98

Cao LG, et.al., Phys.Rev. C89, 044314 (2014)

Summary and perspective

•Microscopic particle-vibration coupling calculations are now available - based on the self-consistent use of nonrelativistic functionals.

• Results for single-particle states are improved compared to mean-field results.

•The effective mass is enchanced by particle-vibration copuling calculations, so the level density is improved around the Fermi surface which is improtant for astrophysics study. The spectroscopic factor is quched by about 20%.

• other contributions, such as the spin-isopsin channels.

• Microscopic optical potential for finite nuclei.

谢谢！